Design, build and data acquisition of atmospheric turbulence using drones

Gihyun Kim* · Supervisor: Prof. Chun-Ho Liu

Department of Mechanical Engineering, The University of Hong Kong, Pokfulam Road, Hong Kong

* ghkim1106@connect.hku.hk

INTRODUCTION

The atmospheric boundary layer is defined as the part of the atmosphere that interacts with the ground, and the momentum, heat, and pollutants exchanged across it are carried mostly by turbulence rather than by the smooth average flow. The major limitation of the meteorological tower is structural: a mast samples data at a fixed height and location, is immobile after deployment, and costs enough to rarely form a network. The field has responded by designing larger aircraft, with the sonic anemometer slung below the drone or installed on a mast and pole placed several tens of centimeters away from the rotor flow on airframes thus weighing from five to nearly thirty kilograms, which are heavy, costly, and subject to stricter flight regulations.

Objective

Instead of increasing the size of the aircraft in order to accommodate the correctly placed sensor, this study proposes keeping the consumer airframe and accepts the resulting limitations. Here we present a drone-mounted sonic anemometer mounted on a 915 g quadcopter, tested in still air at ten different distances from the rotor flow, performed in stepped altitude profiles up to 120 meters.

DRONE-MOUNTED SONIC ANEMOMETER DESIGN

A LI-550 TriSonica Mini ultrasonic anemometer is held at the top of a vertical carbon-fiber rod attached to a 3D-printed tray, designed using SolidWorks, on the upper side of a DJI Mavic 3E drone alongside a custom-printed circuit board (PCB), which logs the flight test data from the anemometer into a dedicated storage unit. The battery is hung at the bottom of the drone, allowing the instrument to log continuously without drawing power from the aircraft. The carbon-fiber rod is 17.5cm long, making the total length from the center of the anemometer to the propellers 30cm.

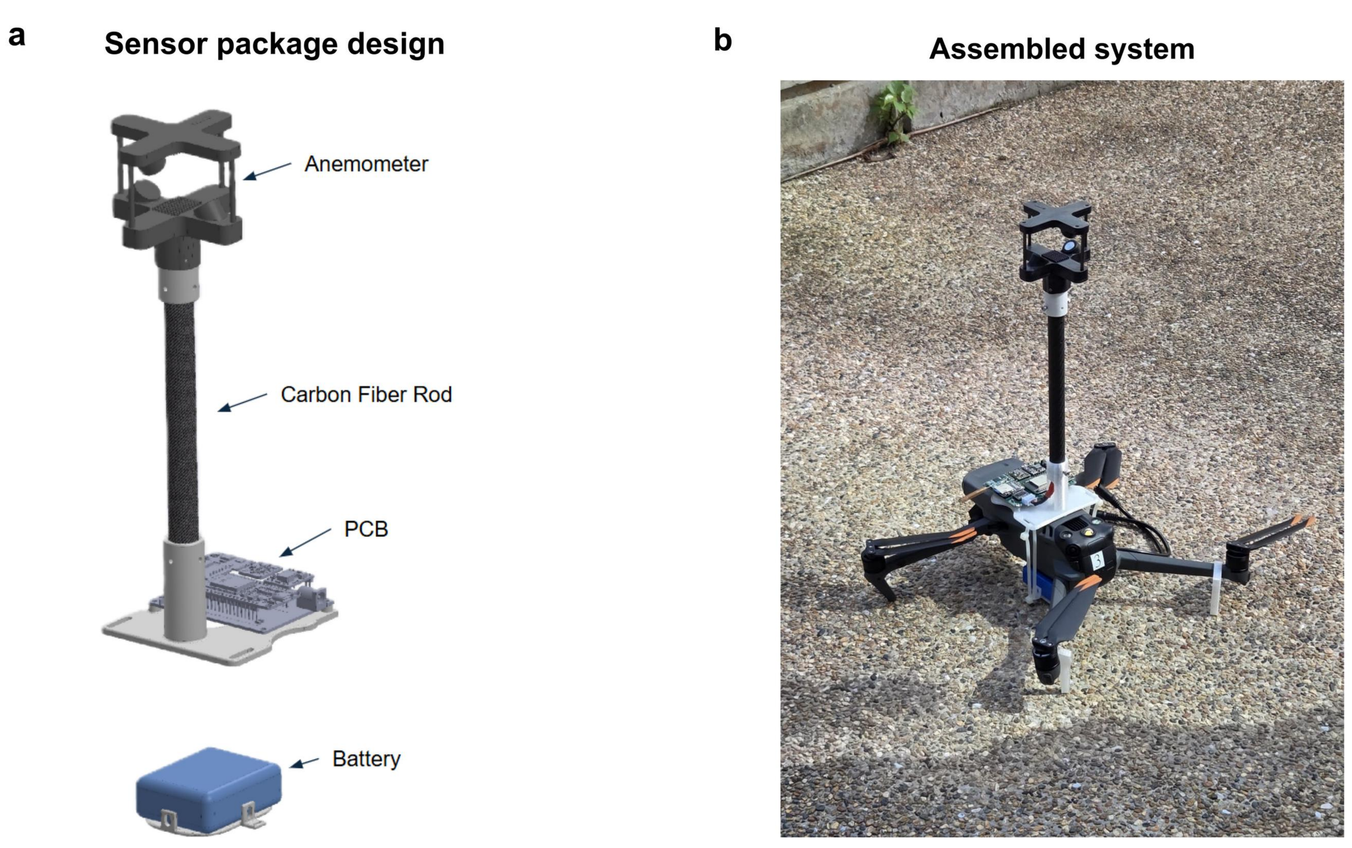

Fig. 2 a, The sensor package: anemometer, carbon-fiber rod, custom PCB, and battery. b, The assembled system on the DJI Mavic 3E.

1,243 g	**328.3 g**	**17.5 cm**	**40 Hz**	**20–120 m**	**2 flights**
total weight	sensor package	rod length	sampling rate	altitudes flown	10 am and 3 pm

ROTOR-INDUCED FLOW AND ROD LENGTH SELECTION

The drone was placed to hover at approximately 3 m inside a large closed space, where the true wind is close to zero; hence, any variation from the baseline was deemed to be the propeller-induced flow measured by the anemometer. A continuous record was collected for each of the ten rods with lengths varying from 5 cm to 30 cm. The minimum for the flight test case was 0.516 m s⁻¹ from the rod distance of 17.5 cm. Rod lengths over 20 cm caused the aircraft to be unstable during flight, which is why the 30 cm row represents only 8.1 s of data.

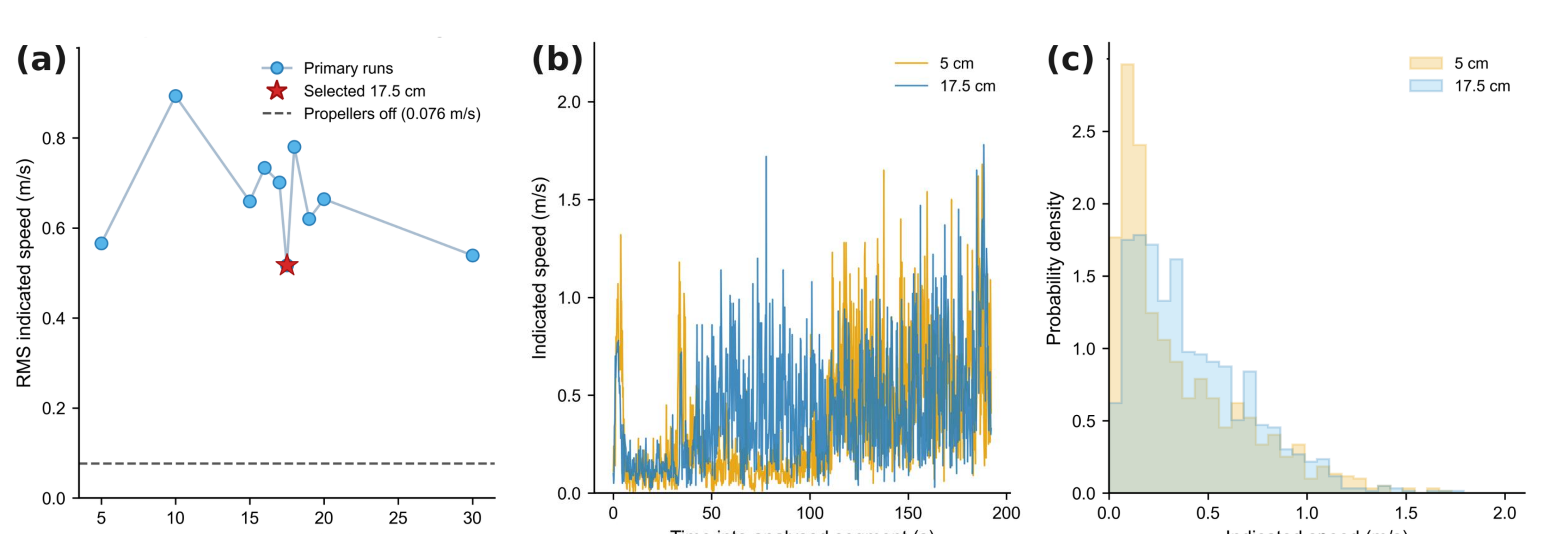

Fig. 3 a, RMS indicated speed for the ten propellers-on runs; the star marks the 17.5 cm configuration used outdoors and the dashed line the measured propellers-off background. b, Indicated speed over time for the 5 cm and 17.5 cm runs. c, The same two runs as distributions.

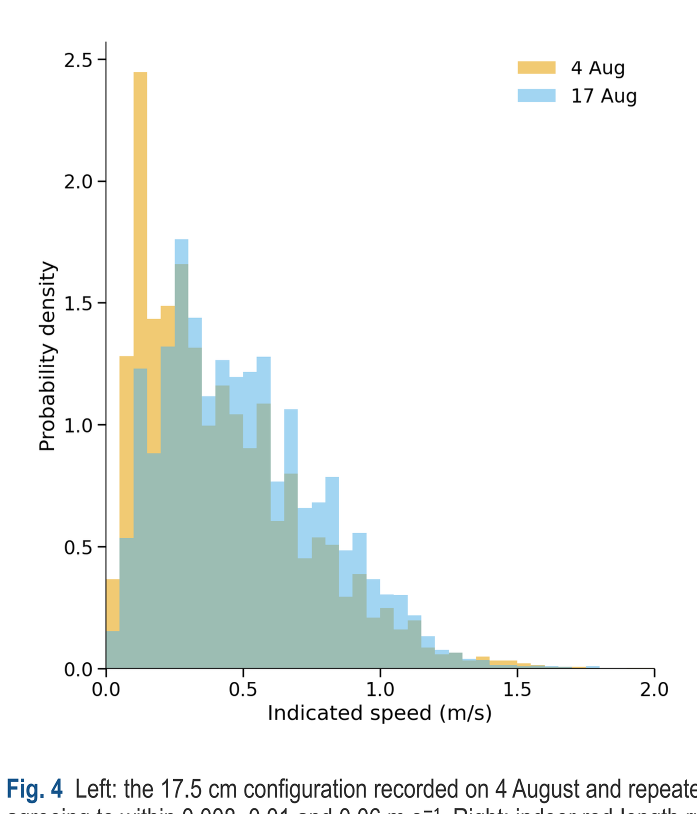

Rod	Mean	s.d.	RMS
5.0	0.414	0.385	0.565
10.0	0.762	0.477	0.899
15.0	0.564	0.342	0.660
16.0	0.638	0.370	0.737
17.0	0.604	0.361	0.704
17.5	**0.421**	**0.298**	**0.516**
18.0	0.688	0.376	0.784
19.0	0.534	0.319	0.622
20.0	0.586	0.321	0.668
30.0	0.488	0.253	0.550
off	0.066	0.038	0.0765

Fig. 4 Left: the 17.5 cm configuration recorded on 4 August and repeated on 17 August, as distributions — standard deviation, interquartile range and 99th percentile all agreeing to within 0.008, 0.01 and 0.06 m s⁻¹. Right: indoor rod-length runs and the propellers-off background; each row is one continuous hover at approximately 3 m, in m s⁻¹.

WIND PROFILES IN THE LOWER BOUNDARY LAYER

For the outdoor flight sessions, the wind profiles at heights 40, 60, 80, 100 and 120 meters above ground, followed by 20 meters, were measured in that order with the drone holding steady flight for approximately 5 minutes at each altitude. This procedure was carried out twice on the same day at 10:00 and 15:00 Hong Kong Time.

Neither profile is shown to increase monotonically with height, with the morning record decreasing between 100 and 120 m and the afternoon record showing a slight decrease from 60 to 80 m. The largest discrepancies between the two sequences occur at 80 and 100 m, where the flights differ by 2.04 and 1.80 m s⁻¹ respectively. The streamwise channel explains the height dependency, with its increase from −1.83 m s⁻¹ at 20 m to −6.61 m s⁻¹ at 120 m.

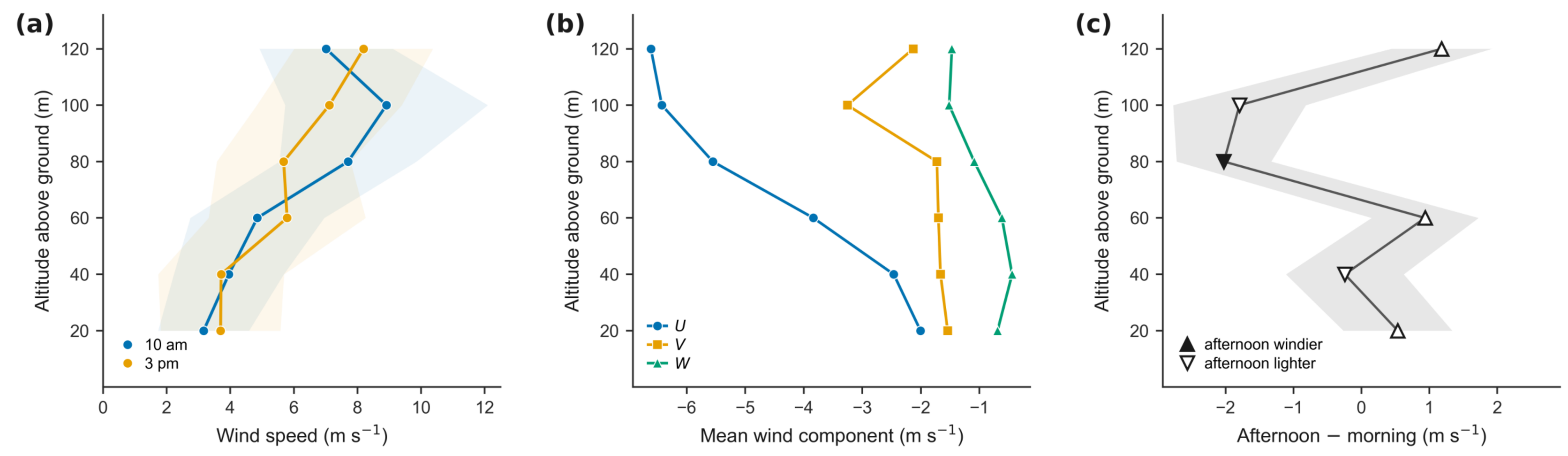

Fig. 5 a, Mean three-dimensional speed magnitude at each nominal hover height for the morning and afternoon flights; shaded bands are one standard deviation of the readings within that hover. b, Mean velocity components across the two sessions against height, in the sensor's own frame of reference. c, Afternoon minus morning, with a band from the combined standard error of the two hover means.

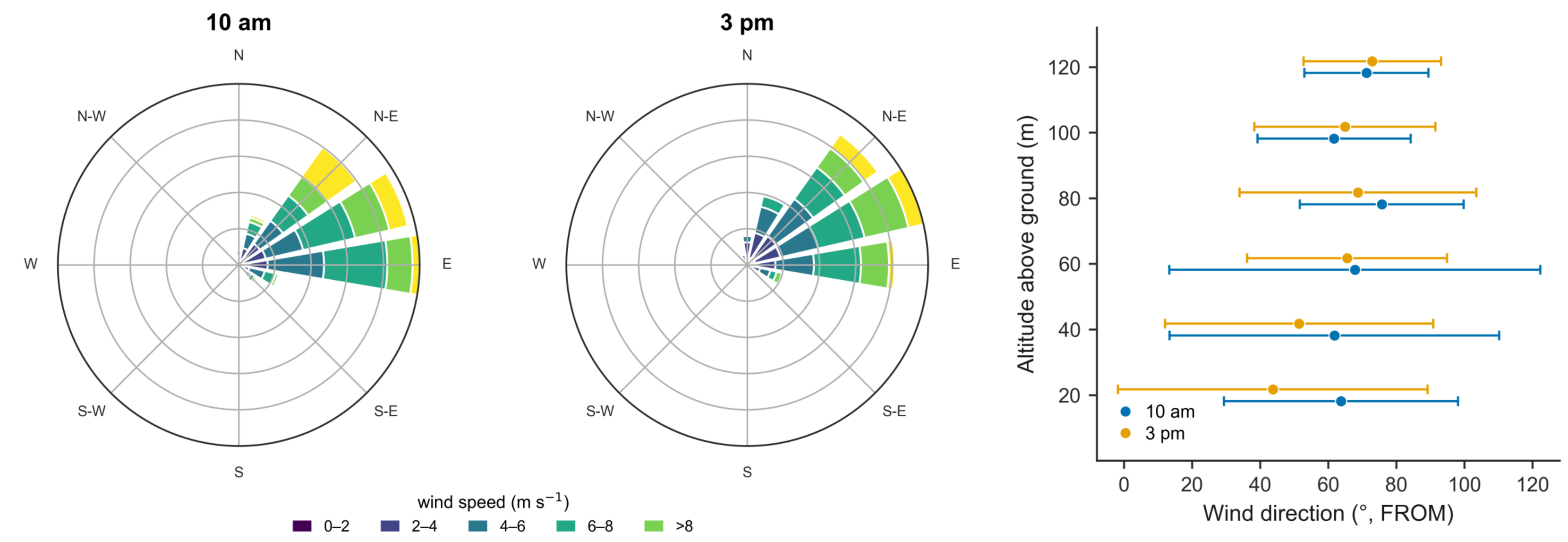

Fig. 6 Left: wind roses for the two sessions, pooled over all six hovers; petal length is the share of samples arriving from that sector and colour is the speed bin. Right: speed-weighted prevailing direction with circular spread at each height.

TURBULENCE STATISTICS AND DATA ANALYSIS

Each hover is centred on its own mean and scaled by its own standard deviation, such that the six altitudes may be overlaid. In the morning, the distributions are positively skewed, with skewness values lying between 0.564 and 1.461, and all carry tails heavier than Gaussian, with kurtosis between 3.34 and 7.28. The afternoon distributions show weaker skewness and kurtosis, with skewness falling to 0.07 at 100 m and kurtosis to 2.55 at 60 m. Therefore, intermittent gusts appear to be characteristic of the morning record but not of the platform or the site itself. Least-squares fits for data between 0.2 to 2.5 Hz yielded a slope range of −1.17 to −1.58 in the morning and between −1.21 and −1.51 in the afternoon; both records therefore decay in a manner consistent with developed turbulence.

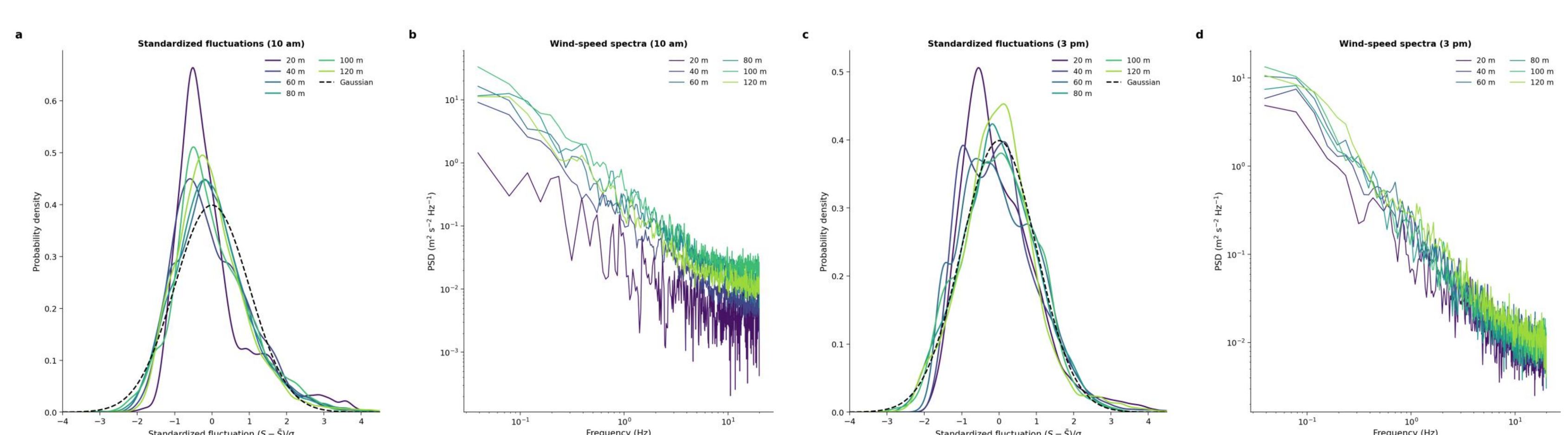

Fig. 7 a, Distributions of standardised wind-speed fluctuations for the morning holds, with a unit Gaussian for comparison. b, Welch power spectra for the same holds. c, d, The corresponding distributions and spectra for the afternoon holds.

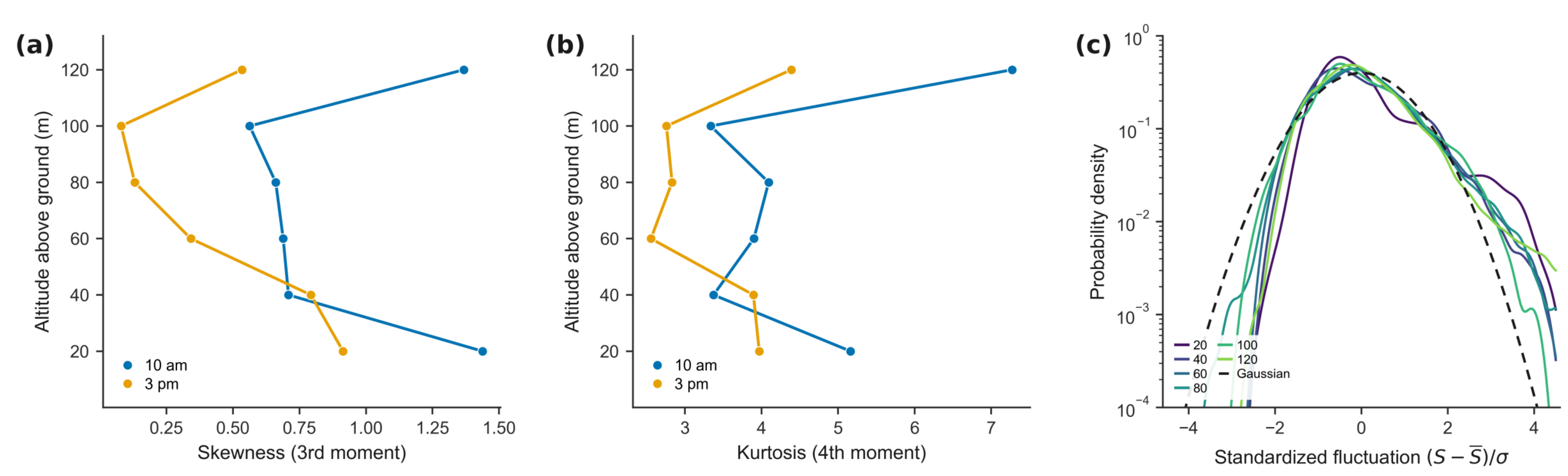

Fig. 8 a, Skewness and b, Pearson kurtosis of the raw speed in each hover against height, for both sessions; a Gaussian would sit at 0 and 3. c, The six standardised distributions overlaid on a unit Gaussian.

CONCLUSION AND LIMITATIONS

Analysis has shown that there exists an interference flux created by the propellers that causes measurements to deviate significantly from the idle state. The smallest interference flux was noted in the 17.5 centimeter model, whose dispersion properties were also reproduced accurately within 0.06 m/s during repeatability tests. Wind velocities increased at greater elevations, exhibiting positive skewness and thick tails in the morning hours, transitioning into a Gaussian-like distribution in the afternoon.

First, the indoor value may not be a truly accurate figure, since the absence of a reference anemometer causes aggregation of PIF, ambient air flow, vibration, aircraft motion, and sensor noise, all into a single measurement. Second, out of nine possible intervals, eight are below the 0.064 m s⁻¹ difference for the 17.5 cm measurement in different test sessions. Third, each flight configuration was performed once in the same altitude order, making it impossible to distinguish the effect of temporal evolution from the height dependency. Addressing these would necessitate another test campaign alongside a calibrated reference anemometer.

SUPPORTING MATERIALS

Carried out under the Laidlaw Undergraduate Research and Leadership Scholarship at HKU. Thanks to Prof. C. H. Liu for supervision and the Faculty of Engineering for support.

Key references: Soltaninezhad et al., Meteorol. Appl. 32, e70065 (2025) · Jin et al., AMT 17, 2721 (2024) · Ghirardelli et al., AMT 18, 2103 (2025) · Kaimal et al., QJRMS 98, 563 (1972).